LIGHT STERILE NEUTRINOS AS DARK-RADIATION CANDIDATES

IRENE TAMBORRA
Max-Planck-Institut für Physik (Werner-Heisenberg-Institut), Föhringer Ring 6, 80805 München, Germany

Recent cosmological data hint towards the existence of additional radiation beyond three active neutrinos and photons (the so-called "dark radiation"). The role of sterile neutrinos as dark-radiation candidates is reviewed at the light of the most recent cosmological constraints.

1 Introduction

Sterile neutrinos are hypothetical $SU(2) \times U(1)$ singlets. They are supposed to mix with one or more active neutrino states, without interacting with any other particle. Low-mass sterile neutrinos have been invoked to explain the excess of $\bar{\nu}_e$ events in the LSND experiment [1] (lately also constrained by the ICARUS collaboration [2]) and the MiniBooNE events [3]. Moreover, short-baseline oscillation experiments (SBL), as well as reactor neutrino flux measurements, seem to hint at the existence of one or even two sterile neutrino families with eV-mass [4,5,6,7]. See [8] for more details and references therein.

At the same time, cosmological data suggest a trend towards the existence of "dark radiation" (i.e., radiation in excess with respect to the three neutrino families and photons) [9,10]. The radiation content of the universe is usually parametrized in terms of the effective number of thermally excited neutrino species ($N_{\rm eff}$) and its standard value is $N_{\rm eff} = 3.046$, slightly exceeding 3 because of e^+e^- annihilation providing residual neutrino heating. Latest constraints on $N_{\rm eff}$, coming from data from the cosmic microwave background anisotropies (CMB) and big-bang nucleosynthesis (BBN), point towards $N_{\rm eff} > 3$.

The Wilkinson Microwave Anisotropy Probe (WMAP) collaboration lately found $N_{\rm eff} = 3.84 \pm 0.4$ combining WMAP-9+CMB+H_0+BAO (where BAO stands for baryon acoustic oscillations and H_0 is the Hubble parameter) [11]. In the last year, new other CMB constraints on $N_{\rm eff}$ have been released by the South Pole Telescope (SPT) [12] and the Atacama Cosmology Telescope (ACT) [13], bringing to an unclear dark-radiation scenario: the WMAP-9 and SPT data both confirm the presence of a dark-radiation component, while the ACT data seem to point towards a value of $N_{\rm eff}$ in agreement with the standard model prediction. No definitive answer about this issue has been provided by the data recently released by the Planck mission [14]. Independently from CMB data, BBN data suggest higher ^{4}He abundance than in the past, interpretable in terms of additional radiation.

Low-mass sterile neutrinos have been adopted to explain such excess [8], although other candidates might be also considered. Concerning the mass and the number of the extra-neutrino families, CMB and BBN in combination favor an excess of radiation compatible with one fully thermalized family of sub-eV sterile neutrinos [15,16]. On the other hand, eV-mass sterile neutrinos, required to explain SBL and reactor anomalies, are cosmologically viable only if additional ingredients are included or partial thermalization of the sterile states is allowed [17].

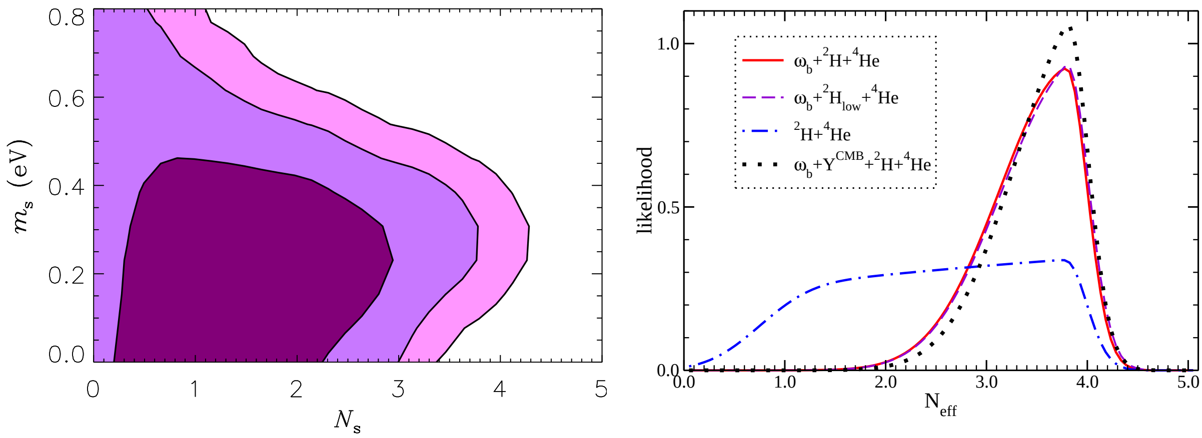

Figure 1: Left: 2D marginalized 68%, 95% and 99% credible regions for the neutrino mass and thermally excited number of sterile families $N_s = N_{\rm eff} - 3.046$, assuming ordinary neutrinos have $m_\nu = 0$ while sterile states have a common mass scale m_s. Plot taken from Hamann et al. (2010) [15]. Right: Marginalized 1-D likelihood functions as a function of $N_{\rm eff}$ using the different combinations of data sets as in the legend. In all cases $N_{\rm eff} > 3$ is favored. Plot taken from Mangano and Serpico (2011) [24].

After reviewing present cosmological bounds for sub-eV and eV mass sterile neutrinos, we will show as an agreement between data coming from SBL experiments and cosmological surveys can be found allowing partial thermalization of the sterile states. We will also discuss as thermalization of sterile neutrinos in the early universe can be prevented assuming an initial leptonic asymmetry much larger than the baryonic one.

2 Cosmological Bounds: Sterile Neutrinos with Sub-eV Mass

From the point of view of cosmology there is no difference between active and sterile neutrinos, provided they are fully thermalized. In fact only the total sum of neutrino masses and the total (effective) number of neutrino species are relevant parameters. However, it is also possible that the sterile states are partially thermalized (as we will see in the following). The contribution of massive neutrinos to the total energy budget of the universe is:

$$\Omega_\nu h^2 = \frac{\sum m_\nu}{91.14 \mathrm{eV}} \ , \tag{1}$$

with $\sum m_\nu = N_s \times m_s$ under the hypothesis $m_\nu = 0$ and being $N_s = N_{\rm eff} - 3.046$.

Using CMB data from WMAP-7 [18], as well as from the ACBAR [19], BICEP [20], QuAD [21] experiments, the halo power spectrum from the SDSS-DR7 luminous red galaxy sample [22], and a prior on the Hubble parameter based on the Hubble Space Telescope observations [23], present cosmological data have been fitted within a standard "vanilla" ΛCDM model allowing more that three neutrino families [15]. The results are shown in Fig. 1 (left panel) in the case of massless active neutrinos ($m_\nu = 0$) and degenerate sterile neutrinos with mass m_s [15]. One or even two sterile neutrino families are allowed by cosmological data and, as the number of sterile families decreases, heavier states are allowed. Note that such data do not favor eV-mass sterile neutrinos since they would violate hot dark matter constraints [17].

Big Bang Nucleosynthesis constrains the number of allowed families under the assumption that they are fully thermalized. It favors up to one fully thermalized extra sterile family [15,17,24] as can be clearly seen in Fig. 1 (right panel). In conclusion, cosmological data are in agreement with the existence of one extra family of fully thermalized sterile neutrinos with sub-eV mass.

3 Cosmological Bounds: Sterile Neutrinos with eV Masses

Sterile neutrinos with eV-mass are favored by SBL experiments and reactors. In this section, we show as one could consider partially thermalized sterile states, in order to find an agreement between SBL and cosmological constraints.

Since eV-mass sterile neutrinos would violate hot dark matter bounds [17,25], we introduce an extension of the classical ΛCDM model by introducing a hot dark matter component in the form of massive neutrinos (Λ Mixed Dark Matter Model, ΛMDM). In order to allow partially-thermalized species, we define

$$N_i = \frac{n_i}{n_i^{\rm th}} \ , \tag{2}$$

where n_i denotes the actual number density of a sterile neutrino with mass m_i and $n_i^{\rm th}$ the number density of a standard fully thermalized neutrino with a Fermi-Dirac phase-space distribution and mass m_i. Therefore, the parameter $N_i \in [0, 1]$ and it defines the fractional contribution of non-standard thermalized sterile states to the dark matter energy density.

Assuming that N_i is independent from the mass m_i, Eq. 1 becomes respectively in a $(3+1)$ or $(3+2)$ scenarios

$$\sum m_\nu = N_4 \times m_4 \text{ and } \sum \mathrm{m}_\nu = \mathrm{N}_4 \times \mathrm{m}_4 + \mathrm{N}_5 \times \mathrm{m}_5 \ , \tag{3}$$

assuming massless active neutrinos.

A joint analysis (cosmological and SBL data) can be done in order to find regions of the parameter space where the two sets of data are in agreement. Including CMB dataset information (from WMAP-9 [26] and SPT [12]), information on the matter power spectrum coming from large scale structures (SDSS-DR7 [22]) as well as $\nu_\mu \to \nu_e$ and $\bar{\nu}_\mu \to \bar{\nu}_e$ appearance data from LSND, KARMEN, NOMAD, MiniBooNE, and ICARUS, ν_e and $\bar{\nu}_e$ disappearance data which take into account the Gallium anomaly and constraints on ν_μ and $\bar{\nu}_\mu$ disappearance obtained from MINOS and SciBooNE and MiniBooNE (see [27] for more details and references therein), a joint analysis has been done in [27], considering both $(3+1)$ and $(3+2)$ scenarios.

The SBL posterior probability on the sterile masses has been included as a prior in the cosmological analysis. As for the $(3+1)$ scenario, results are shown in Fig. 2 (left panel) where the two dimensional marginalized 68% and 95% C.L. regions in the plane (N_4, m_4) are plotted for different combinations of the datasets. When only cosmological data are used, the bounds on N_4 and m_4 are broad, the effect of the SBL data strongly tighten the constraints on the sterile mass, but there is almost no effect on N_4. The best fit values for (N_4, m_4) for (WMAP-9+SPT+SDSS+SBL) are [27]

$$N_4 < 0.83 \ (2\sigma) \ \ \text{and} \ \ \mathrm{m}_4 = 1.23 \pm 0.13 \text{ eV } (1\sigma) \ . \tag{4}$$

Figure 2 (right panel) shows the two-dimensional marginalized 68% and 95% confidence regions in the plane $(N_4 + N_5)$ vs. $(m_4 + m_5)$. It is clear that cosmological and SBL data are consistent with the existence of two extra sterile families, provided they are not fully thermalized. The sum of neutrino masses always shows a clear preference for a non-zero value. In Fig. 2 (right panel) one sees that the cosmological posteriors alone show a preference for a non-zero value for the sum of the masses. The best fit values for (N_4, m_4, N_5, m_5) for (WMAP-9+SPT+SDSS+SBL) are [27]

$$N_4 < 0.85 \ (2\sigma) \quad \text{and} \quad m_4 = 0.95 \pm 0.3 \text{ eV } (1\sigma) \ , \tag{5}$$

$$N_5 < 0.62 \ (2\sigma) \quad \text{and} \quad m_5 = 1.59 \pm 0.49 \text{ eV } (1\sigma) \ . \tag{6}$$

In conclusion, cosmological and SBL data are consistent with the existence of one or even two sterile neutrino families, provided that they are not fully thermalized. Full-standard thermalization ($N_i = 1$, $i = 3, 4$) is not allowed, but fractional occupations as large as ~ 0.9 are possible.

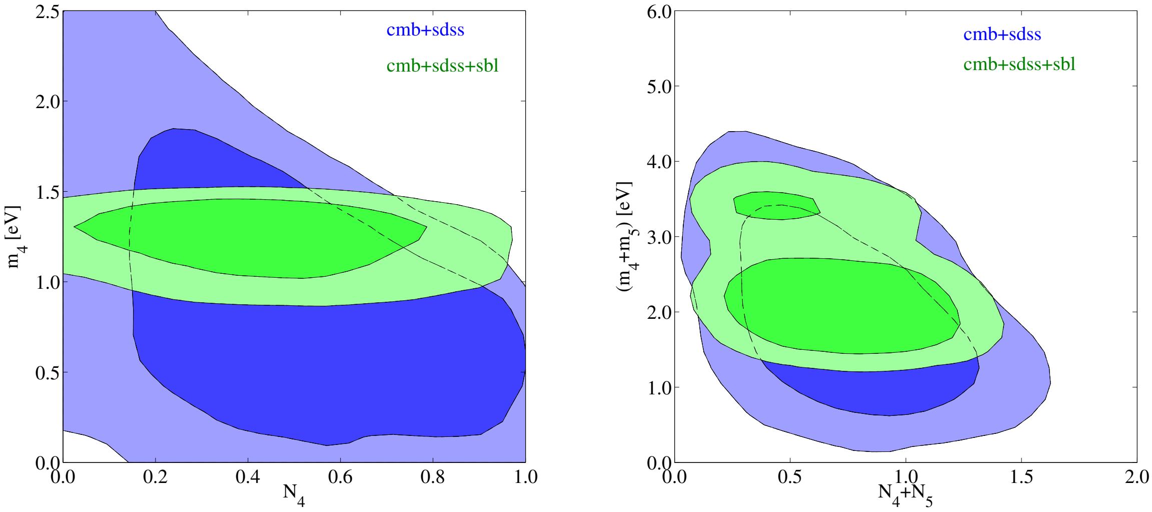

Figure 2: Left: $(3+1)$ analysis – Two dimensional marginalized 68% and 95% confidence level regions in the plane N_4 vs. m_4 for the different combinations of datasets. Right: Reduced $(3+2)$ analysis – Two dimensional marginalized 68% and 95% confidence level regions in the plane (N_4+N_5) vs. (m_4+m_4) for the different combinations of datasets. Plots taken from Achidiacono et al. (2013)[27].

4 How could the thermalization of sterile neutrinos in the early universe be prevented?

Allowing partial thermalization of sterile states, cosmological and SBL data are in agreement. In this Section, studying the evolution of sterile neutrinos up to the BBN temperature (~ 1 MeV), we proof as an initial large leptonic asymmetry prevents thermalization of the sterile states [28].

4.1 Equations of Motion

We consider oscillations of one active flavor ν_a (with $a = e$ or μ, τ) in a sterile neutrino state ν_s separated by a mass difference of δm_s^2 and with a mixing angle in vacuum θ_s (1+1 scheme). Since structure formation data strongly disfavor models with inverted hierarchy and $\delta m_s > 0.2 - 0.3$ eV and cosmological+SBL data require $\mathcal{O}(eV)$ mass sterile sterile states, we will focus on the $\delta m_s^2 > 0$ case (normal hierarchy scenario, NH).

We adopt the density matrix formalism and, for each momentum mode p, decompose the density matrix in terms of the Bloch vector components $(P_0, \mathbf{P}) = (P_0, P_x, P_y, P_z)$ [29],

$$\rho = \frac{1}{2} f_0 (P_0 + \mathbf{P} \cdot \sigma) \ , \qquad \overline{\rho} = \frac{1}{2} f_0 (\overline{P}_0 + \overline{\mathbf{P}} \cdot \sigma) \ , \tag{7}$$

where σ are the Pauli matrices and f_0 is the Fermi-Dirac distribution function with zero chemical potential. The neutrino kinetic equations are:

$$\dot{\mathbf{P}} = \mathbf{V} \times \mathbf{P} - D(P_x \mathbf{x} + P_y \mathbf{y}) + \dot{P}_0 \mathbf{z} \ , \tag{8}$$

$$\dot{P}_0 = \Gamma \left[\frac{f_{\rm eq}}{f_0} - \frac{1}{2}(P_0 + P_z) \right] \ . \tag{9}$$

The dot denotes the time derivative and $f_{\rm eq}$ is the equilibrium distribution. Defining the comoving momentum $x = p/T$ (with T the temperature), the vector $\mathbf{V}$ is a function of the initial leptonic asymmetry $L^{(a)}$, the momentum, and the mass-mixing parameters: $\mathbf{V}(\delta m_s^2, \theta_s, L^{(a)}, x)$. The condition for a matter induced resonance to occur is $V_z = 0$. Since V_z depends on $L^{(a)}$, any non-zero lepton asymmetry can have dramatic consequences for active-sterile neutrino oscillations. The damping term D quantifies the loss of quantum coherence due to ν_a collisions with the background medium. The evolution of P_0 is determined by processes that deplete or enhance

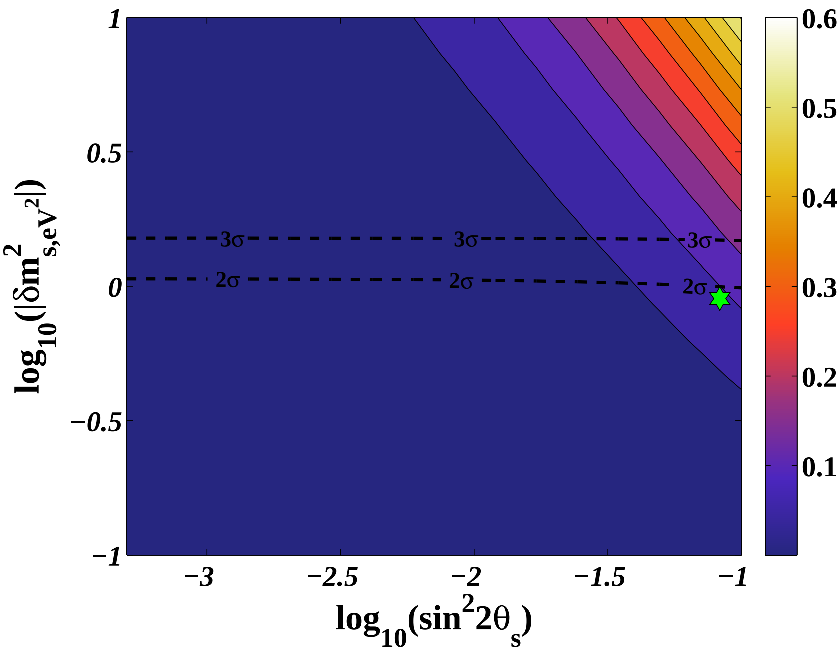

Figure 3: Iso-$\delta N_{\rm eff}$ contours in the $\sin^2 2\theta_s - \delta m_s^2$ plane for $L^{(\mu)} = 10^{-2}$ and $\delta m_s^2 > 0$. The green hexagon denotes the ν_s best-fit mixing parameters as in the $3+1$ global fit in Giunti and Laveder (2011)[30]: $(\delta m_s^2, \sin^2 2\theta_s) = (0.9\ {\rm eV}^2, 0.089)$. The $1-2-3\sigma$ contours denote the CMB+LSS allowed regions for ν_s with sub-eV mass as in Hamman et al. (2010)[15]. Plot taken from Hannestad, Tamborra, Tram (2012) [28].

the abundance of ν_a. The equations of motion for anti-neutrinos can be found by substituting $L^{(a)} = -L^{(a)}$ and $\mu = -\mu$ in the above equations.

4.2 Thermalization for $\delta m_s^2 > 0$ and large initial leptonic asymmetry

An initial large leptonic asymmetry is responsible for blocking the active-sterile flavor conversions by an in-medium suppression of the mixing angle. A large value of $L^{(a)}$ confines the resonances to very small or large values of x, far away from the maximum of the active neutrino momentum distribution. Only at relatively low temperature, the resonance begins to move through the momentum distribution and, for NH, the lepton asymmetry decreases as the resonance moves.

Figure 3 shows the fraction of thermalized neutrinos, $\delta N_{\rm eff}$ for $L^{(\mu)} = 10^{-2}$ for NH. As expected, the production of sterile neutrinos is effectively blocked until after the active species decouples, leading to a very small $\delta N_{\rm eff}$ for the range of mixing parameters studied here. For ν_s mixing parameters as in [30], $\delta N_{\rm eff} \sim 0$ (see green hexagon in Fig. 3). Constraints from BBN, CMB, and LSS have usually assumed a fully thermalized sterile state, but as also mentioned in [15], a finite lepton asymmetry can effectively block thermalization and make this assumption invalid. In that case an eV-mass sterile state are not be in conflict with the cosmological neutrino mass bound.

5 Conclusions

Recent cosmological data favor an excess of radiation beyond three active neutrinos and photons. Light sterile neutrinos are possible candidates. Present data coming from CMB+LSS and BBN point towards the existence of one fully thermalized sub-eV mass sterile family, but do not allow the existence fully thermalized eV-mass sterile neutrinos. However, the full-thermalization hypothesis is not necessarily justified. In fact relaxing this hypothesis, one or even two sterile partially thermalized neutrino families and with $\delta m_s \sim \mathcal{O}(eV)$, as predicted by SBL data, are in agreement with CMB+LSS data. One way to obtain partial thermalization is to assume an initial large leptonic asymmetry.

Acknowledgments

I.T. acknowledges support from the Alexander von Humboldt Foundation and she is grateful to the Rencontres de Moriond EW 2013 organizers for kind hospitality.

References

1. A. Aguilar-Arevalo *et al.* [LSND Collaboration], Phys. Rev. D **64**, 112007 (2001).
2. M. Antonello *et al.*, arXiv:1209.0122 [hep-ex].
3. A. A. Aguilar-Arevalo *et al.* [MiniBooNE Collaboration], Phys. Rev. Lett. **103** (2009) 111801.
4. G. Mention *et al.*, Phys. Rev. D **83**, 073006 (2011).
5. J. Kopp, M. Maltoni and T. Schwetz, Phys. Rev. Lett. **107** (2011) 091801.
6. C. Giunti and M. Laveder, Phys. Rev. D **84** (2011) 093006.
7. G. Karagiorgi, M. H. Shaevitz and J. M. Conrad, arXiv:1202.1024 [hep-ph].
8. K. N. Abazajian *et al.*, arXiv:1204.5379 [hep-ph].
9. J. Hamann *et al.*, JCAP **1007**, 022 (2010).
10. E. Giusarma *et al.*, Phys. Rev. D **85**, 083522 (2012).
11. G. Hinshaw *et al.*, arXiv:1212.5226 [astro-ph.CO].
12. Z. Hou *et al.*, arXiv:1212.6267 [astro-ph.CO].
13. J. L. Sievers *et al.*, arXiv:1301.0824 [astro-ph.CO].
14. P. A. R. Ade *et al.* [Planck Collaboration], arXiv:1303.5076 [astro-ph.CO].
15. J. Hamann *et al.*, Phys. Rev. Lett. **105**, 181301 (2010).
16. E. Giusarma *et al.*, Phys. Rev. D **83**, 115023 (2011).
17. J. Hamann, S. Hannestad, G. G. Raffelt and Y. Y. Y. Wong, JCAP **1109** (2011) 034.
18. E. Komatsu *et al.* [WMAP Collaboration], Astrophys. J. Suppl. **192**, 18 (2011).
19. C. L. Reichardt *et al.*, Astrophys. J. **694** (2009) 1200.
20. H. C. Chiang *et al.*, Astrophys. J. **711** (2010) 1123.
21. M. L. Brown *et al.* [QUaD Collaboration], Astrophys. J. **705** (2009) 978.
22. B. A. Reid *et al.*, Mon. Not. Roy. Astron. Soc. **404** (2010) 60.
23. A. G. Riess *et al.*, Astrophys. J. **699** (2009) 539.
24. G. Mangano and P. D. Serpico, Phys. Lett. B **701** (2011) 296.
25. S. Hannestad, A. Mirizzi, G. G. Raffelt and Y. Y. Y. Wong, JCAP **1008** (2010) 001.
26. C. L. Bennett *et al.*, arXiv:1212.5225 [astro-ph.CO].
27. M. Archidiacono *et al.*, arXiv:1302.6720 [astro-ph.CO].
28. S. Hannestad, I. Tamborra and T. Tram, JCAP **1207**, 025 (2012).
29. G. Sigl and G.G. Raffelt *Nucl. Phys.* B **406** , 423 (1993).
30. C. Giunti and M. Laveder, Phys. Lett. B **706**, 200 (2011) .